Human Molecular Genetics, 2014, Vol. 23, No. 7 ***1677–1686***
doi:10.1093/hmg/ddt557
Advance Access published on November 7, 2013

Membrane damage-induced vesicle–vesicle fusion of dysferlin-containing vesicles in muscle cells requires microtubules and kinesin

Joel R. McDade[1] and Daniel E. Michele[1,2,*]

[1]Department of Molecular & Integrative Physiology, University of Michigan Ann Arbor, MI 48109, USA and [2]Department of Internal Medicine, Division of Molecular Medicine and Genetics, University of Michigan Ann Arbor, MI 48109, USA

Received August 7, 2013; Revised September 24, 2013; Accepted October 30, 2013

Mutations in the dysferlin gene resulting in dysferlin-deficiency lead to limb-girdle muscular dystrophy 2B and Myoshi myopathy in humans. Dysferlin has been proposed as a critical regulator of vesicle-mediated membrane resealing in muscle fibers, and localizes to muscle fiber wounds following sarcolemma damage. Studies in fibroblasts and urchin eggs suggest that trafficking and fusion of intracellular vesicles with the plasma membrane during resealing requires the intracellular cytoskeleton. However, the contribution of dysferlin-containing vesicles to resealing in muscle and the role of the cytoskeleton in regulating dysferlin-containing vesicle biology is unclear. Here, we use live-cell imaging to examine the behavior of dysferlin-containing vesicles following cellular wounding in muscle cells and examine the role of microtubules and kinesin in dysferlin-containing vesicle behavior following wounding. Our data indicate that dysferlin-containing vesicles move along microtubules via the kinesin motor KIF5B in muscle cells. Membrane wounding induces dysferlin-containing vesicle–vesicle fusion and the formation of extremely large cytoplasmic vesicles, and this response depends on both microtubules and functional KIF5B. In non-muscle cell types, lysosomes are critical mediators of membrane resealing, and our data indicate that dysferlin-containing vesicles are capable of fusing with lysosomes following wounding which may contribute to formation of large wound sealing vesicles in muscle cells. Overall, our data provide mechanistic evidence that microtubule-based transport of dysferlin-containing vesicles may be critical for resealing, and highlight a critical role for dysferlin-containing vesicle–vesicle and vesicle–organelle fusion in response to wounding in muscle cells.

INTRODUCTION

Membrane damage is a frequent occurrence in mechanically active tissues, such as skeletal and cardiac muscle, and successful repair of the cell membrane following disruption is critical to muscle function (1–3). Mutations within a critical membrane repair protein, dysferlin, lead to two mild but progressive forms of muscular dystrophy termed limb-girdle muscular dystrophy 2B (LGMD2B) and Myoshi myopathy (MM) (4,5). Dysferlin is a single-pass transmembrane protein containing multiple cytoplasmic C2 domains, and is a member of the evolutionarily conserved ferlin family of proteins. Ferlin proteins play a critical role in membrane fusion across multiple species and cell types (6). Dysferlin appears to have evolved in higher order vertebrates and is relatively muscle specific, with the highest expression in mature skeletal and cardiac muscle (7). Dysferlin is expressed predominantly at or near the plasma membrane in normal adult skeletal muscle, and is markedly mislocalized into the cytoplasm in skeletal muscle from patients with Duchenne muscular dystrophy, as well as LGMDs caused by genetic mutations in genes other than dysferlin (8). Furthermore, combined deficiency of dystrophin and dysferlin worsens disease progression in mice, highlighting the critical role of dysferlin both in normal and diseased skeletal muscle (9). While the functions of dysferlin in muscle that are important for its causal role in muscular dystrophy and the mechanisms of those functions are still unclear, dysferlin has been suggested to play a role in a wide variety of processes related to membrane fusion, including t-tubule biogenesis and maintenance (10), cell–cell fusion (11), cell adhesion (12) and muscle growth (13).

*To whom correspondence should be addressed at: Department of Molecular & Integrative Physiology, University of Michigan, NCRC Bldg 26-207S, 2800 Plymouth Road, Ann Arbor, MI 48109-2800, USA; Department of Internal Medicine, University of Michigan, NCRC Bldg 26-207S, 2800 Plymouth Road, Ann Arbor, MI 48109-2800, USA. Tel: +1 7347645738; Fax: +1 7349368813; Email: dmichele@umich.edu

Perhaps the most intensively studied role for dysferlin is in the process of membrane resealing. Membrane resealing is a conserved process by which cells are able to survive mechanical disruption of the plasma membrane (14–19). Dysferlin-null skeletal and cardiac muscle show enhanced uptake of membrane impermeable dye following laser-induced wounding, suggesting that dysferlin may play a role in membrane resealing (3,20). Dysferlin is enriched at sites of cellular damage, and these 'patches' are devoid of plasma membrane proteins, indicating that dysferlin may have been delivered from an intracellular membrane source (3,20). Electron micrographs of dysferlin-deficient muscle fibers show robust accumulation of vesicles under the sarcolemma, suggesting that in wild-type muscle, dysferlin may play a role in fusion of subsarcolemma vesicles with the plasma membrane and that these vesicles may be critical to repairing the membrane following wounding (3). Although these data are consistent with a role for dysferlin-containing vesicles in membrane resealing in skeletal muscle, exactly how dysferlin-containing vesicles contribute to membrane resealing in muscle cells is not clear.

Current knowledge of membrane resealing is largely derived from studies in the sea urchin egg and fibroblast model systems, which demonstrated that fusion of intracellular vesicles with the plasma membrane is critical for resealing (15–17,21). Dysferlin localizes to the plasma membrane and intracellular vesicles in developing myotubes, and interacts with numerous proteins involved in membrane transport, including caveolin-3 (22, 23), annexin-4 (5), annexin-6 (24), enlargeosomal marker AHNAK (25) and tubulin (26), but the exact contribution of dysferlin-containing vesicles to resealing following wounding remains elusive, as few studies have examined the behavior of dysferlin-containing vesicles in live cells following cellular wounding. Therefore, we sought to investigate the behavior of dysferlin-containing vesicles in live-muscle cells prior to and following wounding, and examine the role of kinesin and microtubules in dysferlin vesicle biology.

We utilized live-cell imaging of L6 myotubes expressing fluorescently tagged dysferlin molecules to study the real-time dynamic behavior of dysferlin-containing vesicles prior to, and following mechanical membrane disruption. Using this approach, we demonstrate that dysferlin-containing vesicles interact with microtubules via plus-end directed kinesin heavy chain motor, KIF5B. In response to membrane damage, dysferlin-containing vesicles undergo rapid vesicle–vesicle and vesicle–organelle fusion with lysosomes to form extremely large cytoplasmic vesicles, in a manner that is dependent on both microtubules and functional KIF5B. These data support the overall hypothesis that the interaction of dysferlin-containing vesicles with microtubules is critical for dysferlin vesicle function following cellular wounding, and implicate lysosomal membranes as potential partners for dysferlin-containing vesicle fusion events following cellular wounding in skeletal muscle.

RESULTS

Dysferlin-eGFP localizes to distinct cytoplasmic vesicles in differentiated L6 myotubes

Fluorescently tagged dysferlin fusion constructs were generated to study the localization and behavior of dysferlin-containing vesicles in cultured skeletal muscle cells. Deconvolution imaging of L6 myotubes transiently expressing dysferlin-eGFP revealed that dysferlin-containing membranes, and vesicles were present in linearly arranged clusters throughout the length of the myotube (Fig. 1A). The exact composition of dysferlin-containing vesicles and whether these vesicles are derived from any known membrane compartments remains to be determined. Antibody labeling of an endoplasmic reticulum marker, protein disulfide isomerase (PDI) (Fig. 1B), as well as a Golgi marker GM130 (Fig. 1C), in dysferlin-eGFP-expressing myotubes was used to examine the relationship between dysferlin-containing vesicles and the secretory pathway in skeletal muscle cells. Dysferlin-eGFP showed minimal overlap with either GM130 or PDI, indicating that dysferlin-containing vesicles are distinct from the secretory pathway. Dysferlin-eGFP and LGP120-mCherry localize to distinct vesicular structures when coexpressed in L6 myotubes, indicating that dysferlin-eGFP does not localize to lysosomes in skeletal muscle cells (Fig. 1D).

Dysferlin-containing vesicles move along microtubules via KIF5B motors in differentiated L6 myotubes

Live-cell imaging of fluorophore-labeled dysferlin expressing L6 myotubes was used to explore the dynamic behavior of dysferlin-containing vesicles, and the relationship between dysferlin-containing vesicles and microtubules as well as

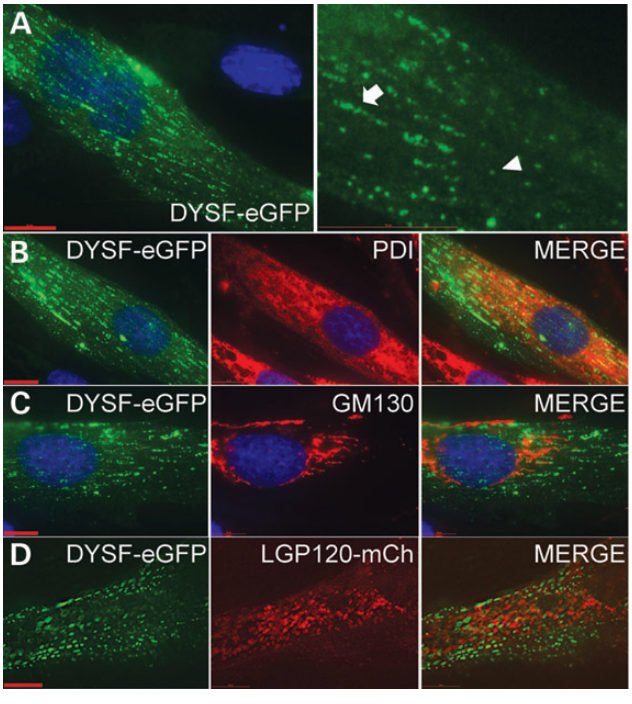

Figure 1. Dysferlin-eGFP localizes to a population of distinct vesicles in differentiated L6 myotubes. (**A**) Dysferlin-containing vesicles are arranged in linear arrays throughout the cytoplasm of L6 myotubes. High magnification of (A) shows that dysferlin-containing vesicles are isolated (arrowhead, right panel), and also accumulate in regularly distributed vesicle clusters (arrow, right panel). Antibody labeling of fixed L6 myotubes shows that cytoplasmic dysferlin-containing vesicles do not colocalize with endogenous ER marker PDI (**B**), or Golgi marker GM130 (**C**). (**D**) Dysferlin-eGFP and lysosomal marker mCherry-LGP120 localize to distinct vesicle populations in differentiated L6 myotubes. Scale bar = 10 μm.

kinesin motors in cultured L6 myotubes. The majority of dysferlin-containing vesicles, particularly those clustered within the cytoplasm or near the membrane, were non-motile over the course of imaging (~2 min) except for occasional back-and-forth movements. However, a portion of dysferlin-containing vesicles moved in linear paths along the longitudinal axis of the myotube up to tens of microns in length at an approximate average rate of 0.63 ± 0.045 μm/s (Fig. 2A, Supplementary Material, Movie S1). Owing to the remarkable length and linearity of dysferlin-containing vesicle movements, we proposed that microtubules may serve as tracks for dysferlin-containing vesicle transport in skeletal muscle. Microtubules were antibody labeled in fixed dysferlin-eGFP-expressing L6 myotubes in order to explore the relationship between dysferlin-containing vesicles and microtubules in skeletal muscle. Microtubule structures arranged in a dense longitudinally oriented lattice that extended throughout the entire myotube, and a portion of dysferlin-containing vesicles were associated with microtubules (Fig. 2B, see inset). To directly assess whether microtubules are required for dysferlin-containing vesicle transport in L6 myotubes, movement of dysferlin-vesicles was analyzed for long-range (>2 μm) vesicle movements in dysferlin-eGFP-expressing L6 myotubes prior to, and following treatment with nocodazole. As shown in Figure 2C, treatment with 750 nM nocodazole clearly disrupted the microtubule lattice and significantly reduced vesicle movements >2 μm in differentiated L6 myotubes (Fig. 2D). We examined whether dysferlin-containing vesicles labeled with ubiquitously expressed kinesin motor KIF5B by imaging L6 myotubes co-expressing dysferlin-mCherry and GFP-KIF5B and analyzed the dynamic movement of each label relative to the other in live skeletal muscle myotubes. Motile and non-motile cytoplasmic dysferlin-containing vesicles are labeled by GFP-KIF5B in L6 myotubes (Fig. 2E, Supplementary Material, Movie S2), but not neuron-specific isoform KIF5C (Supplementary Material, Fig. S1), indicating that dysferlin-containing vesicles contain KIF5B motors in L6 myotubes.

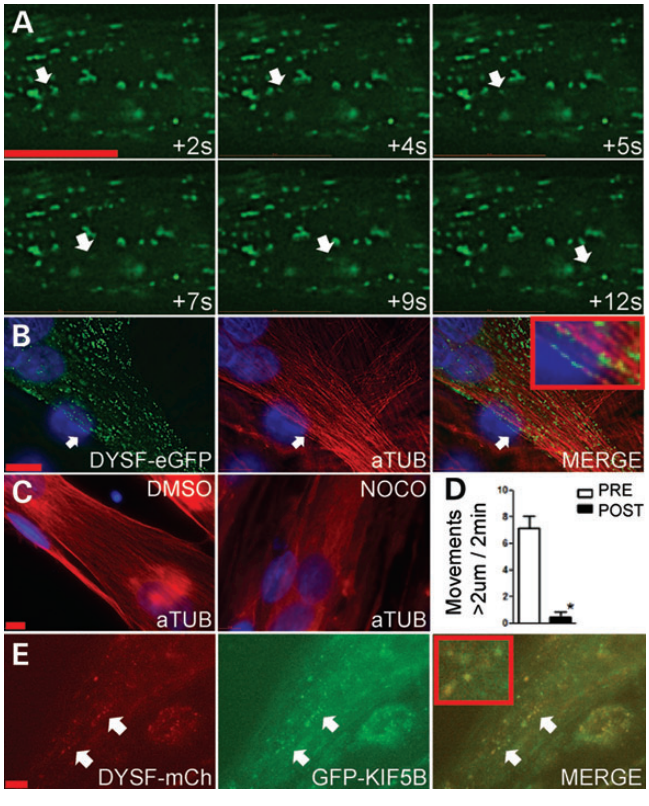

Figure 2. Dysferlin-containing vesicles move along microtubules via KIF5B motors in differentiated L6 myotubes. (**A**) Live-cell imaging of dysferlin-eGFP-expressing L6 myotubes shows that dysferlin-containing vesicles undergo long-range movements along the longitudinal axis of L6 myotubes (Supplementary Material, Movie S1). (**B**) Antibody labeling of α-tubulin in dysferlin-eGFP-expressing L6 myotubes reveals that dysferlin-containing vesicles colocalize with microtubules in L6 myotubes; DAPI = blue. (**C**) Antibody labeling of α-tubulin in differentiated L6 myotubes shows that microtubules form a dense, longitudinally oriented lattice in L6 myotubes (C, left panel) and are disrupted following treatment with a microtubule depolymerizing agent, nocodazole (C, right panel); DAPI = blue. (**D**) Microtubule disruption inhibits long-range movement of dysferlin-containing vesicles in skeletal muscle myotubes. Dysferlin-eGFP-expressing myotubes were imaged 2 min prior to, and following treatment with nocodazole, and vesicle movements >2 μm were quantified for each condition ($n = 13$, $P < 0.001$). (**E**) Both non-motile and motile dysferlin-containing vesicles label with KIF5B motors in skeletal muscle myotubes. Data are representative of 16 cotransfected myotubes (Supplementary Material, Movie S2). Scale bar = 10 μm.

Membrane disruption induces formation of extremely large dysferlin-containing vesicles in L6 myotubes

There have been few studies attempting to directly examine damage-induced fusion of dysferlin-containing vesicles following wounding in living skeletal muscle cells. Therefore, to characterize the response of dysferlin-containing vesicles to membrane disruption in skeletal muscle cells, we used *in vitro* mechanical wounding of dysferlin-eGFP-expressing L6 myotubes in conjunction with live-cell imaging to track the dynamic responses of dysferlin-containing vesicles. Mechanical wounding has been used previously to study the behavior of other repair proteins in muscle cells (27), but the response of dysferlin-containing vesicles to mechanical wounding has not been fully characterized. Prior to wounding, dysferlin-containing vesicles were distributed throughout the cytoplasm of the myotube (Fig. 3A, left). Cellular damage was elicited using a glass-pulled micropipette guided to a precise location on the myotube, and allowed to puncture the membrane. Damage was indicated by (i) loss of GFP-fluorescence in the affected area and (ii) noticeable tactile response, including membrane tearing and subsequent retraction of the myotube. Immediately following disruption, dysferlin-containing vesicles combine to form extremely large cytoplasmic vesicles adjacent to the lesion, and throughout the cytoplasm (Fig. 3A, white arrows, right panel, Supplementary Material, Movie S3). The resulting vesicles varied in size from 1 μm to >10 μm. All vesicles forming following wounding had an apparent lumen, which was not the case for dysferlin-containing vesicles prior to membrane disruption. The time-course of large vesicle formation was rapid, beginning as rapidly as 1 s post-wound and completely formed ~1 min post-wound. Representative time-lapse images of large vesicle formation following wounding is presented in high magnification in Figure 3B, where multiple small vesicles are incorporated into a large vesicle within a time-frame of 1 s to form an incrementally larger vesicle (white arrows, right panel, Supplementary Material, Movie S4). In some instances, damage-induced vesicles collapsed into the adjacent membrane

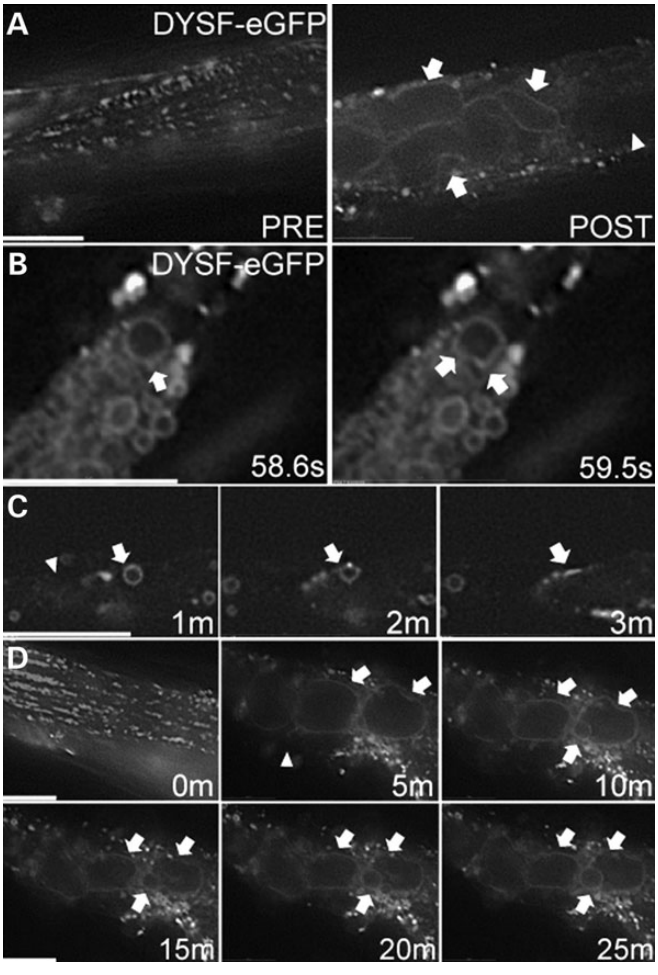

Figure 3. Membrane damage induces fusion of dysferlin-containing vesicles leading to the formation of extremely large vesicles in L6 myotubes. (**A**) Membrane disruption induces the formation of large dysferlin-containing vesicles in L6 myotubes. L6 myotubes expressing dysferlin-eGFP were subjected to live-cell imaging prior to and after membrane disruption with a glass micropipette. Prior to damage, dysferlin-containing vesicles appear regularly distributed throughout the cytoplasm (left panel). Following damage (arrowhead), dysferlin-containing vesicles (shown in left panel) undergo rapid vesicle–vesicle fusion to form extremely large vesicles adjacent to membrane lesion (white arrows) and throughout the cytoplasm (Supplementary Material, Movie S3). (**B**) Large damage-induced dysferlin-containing vesicles result from fusion of smaller dysferlin-containing vesicles in L6 myotubes. Analysis of high magnification, consecutive live-cell images shows small vesicles (arrowheads) undergo fusion with a large vesicle to form an incrementally larger vesicle (Supplementary Material, Movie S4). (**C**) Example of large dysferlin-containing vesicle collapsing with the plasma membrane following membrane disruption (Supplementary Material, Movie S5). (**D**) The majority of damage-induced dysferlin-containing vesicles persist for many minutes following membrane disruption. Scale bar = 10 μm.

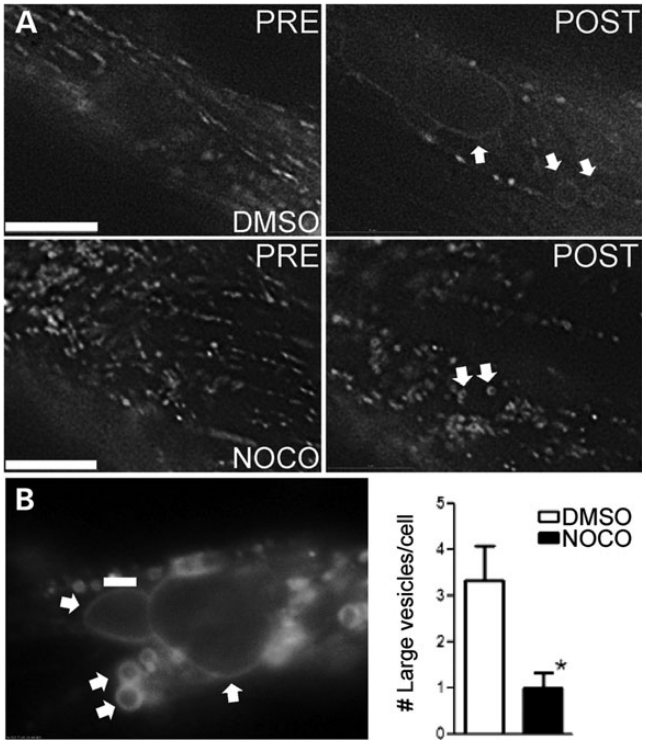

Figure 4. Disruption of microtubules reduces the formation of large dysferlin-containing vesicles following membrane wounding in L6 myotubes. (**A**) Effect of pharmacological inhibition of microtubules on large vesicle formation following wounding in L6 myotubes. Prior to damage, dysferlin-containing vesicles show typical arrangement in linear arrays throughout the cytoplasm of differentiated L6 muscle cells (left panels). In DMSO-treated control cells dysferlin-containing vesicles fuse to form large vesicles following membrane disruption (arrows, top-right panel). Disruption of microtubules by pre-treatment with nocodazole markedly reduces the formation of large dysferlin-containing vesicles following wounding (middle panels). (**B**) Quantification of large dysferlin-containing vesicle formation. The left panel is a representative image showing multiple vesicles (arrows) >2 μm in size (white bar). The total number of large vesicles per cell was quantified for DMSO and nocodazole treatment (bar graph). Treatment with nocodazole significantly reduced the number of large vesicles formed following wounding compared with DMSO control ($n = 15$ cells for DMSO; $n = 9$ cells for nocodazole; $P < 0.05$). See Supplementary Material, Movie S5 (DMSO), and 7 (nocodazole); scale bar = 10 μm.

(Fig. 3C, Supplementary Material, Movie S5), while the vast majority persist many minutes following wounding (Fig. 3D).

Disruption of microtubules but not inhibition of actin–myosin interaction diminishes formation of large dysferlin-containing vesicles following membrane disruption in L6 myotubes

Our data suggest that dysferlin-containing vesicles interact with microtubules and microtubule disruption inhibits vesicle movement. Therefore, the requirement of microtubules for fusion of dysferlin-containing vesicles following wounding in L6 myotubes was examined. Dysferlin-eGFP-expressing L6 myotubes were pre-treated with either DMSO or DMSO + 750 nM nocodazole for ≥30 m and subjected to live-cell imaging prior to, and following membrane disruption. Time-lapse data was analyzed for fusion of dysferlin-containing vesicles and the resulting formation of large vesicles with a visible lumen. Dysferlin-eGFP-expressing L6 myotubes were not affected by pre-treatment with DMSO (Fig. 4A, top-left), and mechanical wounding induced formation of extremely large vesicles in DMSO-treated cells (Fig. 4A, top-right, Supplementary Material, Movie S6). Treatment with nocodazole did not affect dysferlin-containing vesicle localization within the cell prior to wounding (Fig. 4A, middle-left panel), but the formation of large dysferlin-containing vesicles following wounding was significantly reduced (Fig. 4A middle-right panel, quantified in Fig. 4B, Supplementary Material, Movie S7). To determine

whether the inhibitory effect of nocodazole treatment on formation of large dysferlin-containing vesicles was specific for microtubule disruption or due to indirect disruption of actin-based transport, dysferlin-eGFP-expressing L6 cells were acutely treated with a potent and specific non-muscle myosin-II inhibitor, blebbistatin, and assayed for fusion following mechanical wounding. Treatment with 25 μM blebbistatin did not markedly alter dysferlin-containing vesicle localization and did not affect the formation of large dysferlin-containing vesicles following membrane wounding (Supplementary Material, Fig. S2).

Functional KIF5B is required for formation of large dysferlin-containing vesicles following membrane disruption

Our data indicate that KIF5B labels dysferlin-containing vesicles and may be a critical motor protein for movement of dysferlin-containing vesicles along microtubules in skeletal muscle cells. Therefore, over-expression of a dominant negative KIF5B construct was used to examine the role of KIF5B in the formation of large dysferlin-containing vesicles following mechanical wounding in L6 myotubes. The dominant negative KIF5B encodes a 'headless' truncation mutant of KIF5B, which contains half of the stalk domain and cargo-binding domain, but lacks a functional motor domain. Deconvolution imaging of fixed L6 myotubes expressing dysferlin-eGFP and either wild-type mCherry-labeled KIF5C (mCherry-wtKIF5) or mCherry-labeled-dominant negative mutant of KIF5B (mCherry-dnKIF5), revealed that localization of dysferlin-containing vesicles was not markedly affected by expression of either construct (Fig. 5A). Genomic deletion of KIF5B has been reported to disrupt organization of the Golgi complex, actin-cytoskeleton, and lysosomes in KIF5B-null myoblasts (28, 29). Therefore, we examined whether expression of dnKIF5 affected the Golgi complex, actin-cytoskeleton and lysosomes in differentiated L6 myotubes. Over-expression of dnKIF5 did not disrupt the actin-cytoskeleton or the Golgi complex in L6 myotubes (Supplementary Material, Fig. S3A, B). Lysosomal organization was not affected by expression of dnKIF5, as most lamp-1 positive structures were dispersed throughout the cytoplasm of wtKIF5- and dnKIF5-expressing cells (Supplementary Material, Fig. S3C). To examine the role of KIF5B in the formation of large dysferlin-vesicles, myotubes co-expressing either dysferlin-eGFP and mCherry-wtKIF5 (Fig. 5B, top-left panel) or dysferlin-eGFP and mCherry-dnKIF5 (Fig. 5B, bottom-left panel) were subjected to mechanical wounding and assayed for the formation of large dysferlin-containing vesicles. Expression of mCherry-wtKIF5 did not affect the behavior of dysferlin-containing vesicles following wounding as membrane disruption induced the formation of large dysferlin vesicles adjacent to the lesion site (Fig. 5B, top-right, and Supplementary Material, Movie S8). Expression of mCherry-dnKIF5 significantly reduced the formation of large dysferlin-containing vesicles following wounding, indicating that functional KIF5B is required for formation of large dysferlin-containing vesicles following wounding in skeletal muscle cells (Fig. 5B, bottom-right panel, quantified in Fig. 5C and Supplementary Material, Movie S9).

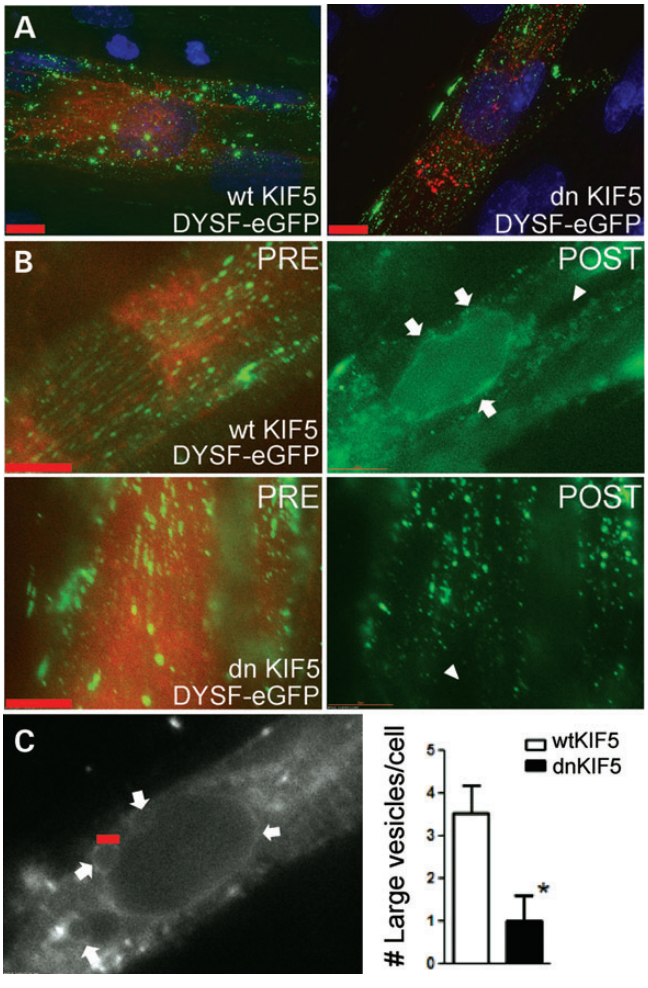

Figure 5. Expression of dnKIF5 inhibits formation of large dysferlin-containing vesicles following membrane wounding in L6 myotubes. (**A**) Expression of dominant negative KIF5 does not dramatically alter dysferlin-containing vesicle localization in L6 myotubes. Representative deconvolved images of fixed L6 myotubes co-expressing dysferlin-eGFP (green) and either mCherry-labeled wtKIF5 (left, red) or mCherry-labeled dnKIF5 (right, red); DAPI = blue. (**B**) Dominant negative KIF5 inhibits formation of large dysferlin-containing vesicles following membrane disruption in L6 myotubes. L6 myotubes expressing dysferlin-eGFP and mCherry-wtKIF5 control or mCherry-dnKIF5 constructs were analyzed prior to (left panels) and following mechanical wounding (right panels) using live-cell imaging. Formation of damage-induced large dysferlin vesicles is diminished in dnKIF5 expressing (bottom-right) but not wtKIF5 expressing myotubes (arrows, top-right). (**C**) Quantification of large dysferlin-containing vesicle formation. The left panel is a representative image showing multiple vesicles (arrows) >2 μm in size (red bar). The total number of large vesicles per cell was quantified for myotubes expressing dysferlin-eGFP with mCherry-wtKIF5 or mCherry-dnKIF5 (bar graph). Expression of dnKIF5 significantly reduces the formation of large dysferlin-containing vesicles following mechanical disruption in L6 myotubes. wtKIF5 $n = 13$ cells, dnKIF5 $n = 10$ cells; $P < 0.05$. Supplementary Material, Movie S8 (wtKIF5) and 9 (dnKIF5); scale bar = 10 μm.

Dysferlin-containing vesicles undergo heterotypic fusion with lysosomes following mechanical wounding in differentiated L6 myotubes

Lysosomes are thought to undergo exocytosis in response to membrane wounding, and have been implicated in membrane resealing in non-muscle cell systems (30). Interestingly,

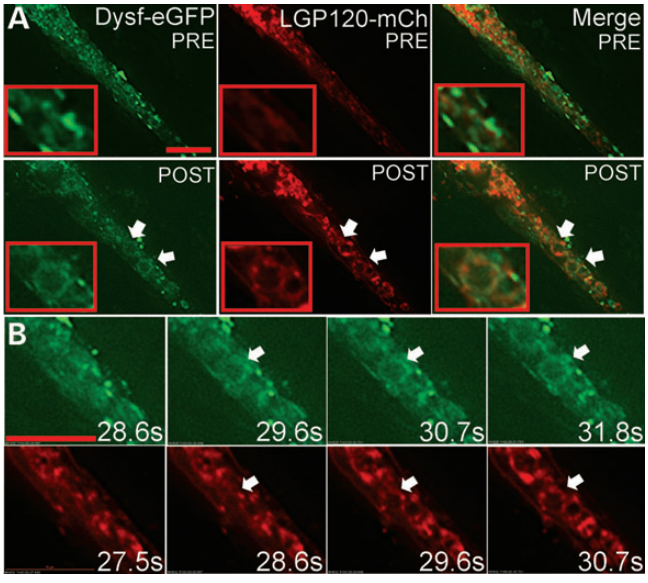

Figure 6. Dysferlin-eGFP interacts with lysosomal membranes following mechanical wounding in differentiated L6 cells. (**A**) Dysferlin-eGFP and LGP120-mCh occupy distinct compartments in unwounded L6 myotubes (top panels), and form large colabeled cytosolic vesicles following mechanical wounding (bottom panels). (**B**) High magnification time-lapse imaging of dysferlin-eGFP (top panels, starting from left) and LGP120-mCh (bottom panels, starting from left) from cell shown in panel (A). Small interspersed dysferlin-containing vesicles and LGP120-containing membranes undergo heterotypic fusion to form a large vesicle adjacent to the membrane lesion (time indicated is time post-wounding). See Supplementary Material, Movie S10. Scale bar = 10 μm.

lysosomal marker LAMP-2 is mislocalized in dysferlin-null myoblasts indicating a possible defect in lysosomal transport (13), but whether lysosomal compartments interact with dysferlin vesicles in muscle cells is not known. To address this, L6 myotubes co-expressing dysferlin-eGFP and LGP120-mCherry (LGP120-mCh) were subjected to live-cell imaging prior to, and following mechanical wounding and the extent of co-labeling was analyzed. Prior to membrane wounding, dysferlin-eGFP and LGP120-mCh label independent vesicle populations with minimal overlap (Fig. 6A, top panels). Large co-labeled structures form following mechanical wounding, indicating that dysferlin-containing vesicles are capable of fusion with lysosomal compartments in L6 myotubes following cellular wounding (Fig. 6A, bottom panels). High magnification time-lapse images of heterotypic dysferlin/lysosome vesicle formation are shown in Figure 6B and Supplementary Material, Movie S10.

DISCUSSION

Dysferlin is a critical component of the membrane repair machinery in both skeletal and cardiac muscle (3,20), and loss of this protein leads to muscular dystrophy (3,31,32). Dysferlin-containing vesicles are thought to play a critical role in muscle resealing, but there have been very few studies attempting to directly examine the behavior of dysferlin-containing vesicles in live-muscle cells in the context of cellular wounding. Studies from non-muscle model systems suggest that microtubule-based transport of intracellular vesicles is critical for resealing (15,21), but the role of microtubules and kinesin motors in dysferlin-mediated membrane repair in muscle remains unexplored. Therefore, the aim of this study was to examine the behavior of dysferlin-containing vesicles under normal conditions and following cellular wounding in muscle cells, and test the hypothesis that microtubules and kinesin are required for dysferlin-containing vesicle function in muscle cells. Owing to the dynamic nature of vesicle transport/fusion and membrane resealing, we used a live-cell imaging approach to study dysferlin-containing vesicles in unperturbed and mechanically wounded myotubes. This approach allowed for the resolution of individual vesicle movements and direct visualization of vesicle fusion events following cellular wounding in live-muscle cells. Our data show that dysferlin-containing vesicles are transported along microtubles via kinesin heavy chain isoform KIF5B, and undergo rapid microtubule- and KIF5B-dependent fusion to form extremely large vesicles following cellular wounding in skeletal muscle cells. Furthermore, we identify lysosomal compartments as potential interacting partners of dysferlin-containing vesicles following cellular wounding in skeletal muscle cells.

Dysferlin-containing vesicles move along microtubules via KIF5B in skeletal muscle cells

Antibody labeling of microtubules in fixed dysferlin-eGFP-expressing L6 myotubes revealed that dysferlin-containing vesicles are arranged along longitudinally oriented microtubule structures. Live-cell imaging of dysferlin-eGFP-expressing L6 myotubes showed that the majority of dysferlin-containing membranes are arranged in non-motile vesicle clusters, with a small fraction of dysferlin-containing vesicles undergoing microtubule-dependent long-range movement. Kinesin heavy chain has been implicated in damage-induced exocytosis of vesicles in other model systems (15,17), and a study that screened for dysferlin interacting proteins using mass spectrometry identified ubiquitous kinesin motor KIF5B (33). Consistent with a role for KIF5B on dysferlin-containing vesicles, live-cell imaging of L6 myotubes expressing dysferlin-mCh and eGFP-KIF5B revealed that dysferlin-containing vesicles are labeled by KIF5B, and co-labeled vesicles are capable of long-range movements. Furthermore, the measured velocity of motile dysferlin-containing vesicles is in the range of velocities reported for mitochondria in neurons (34), and kinesin motors in COS cells (35). Interestingly, most KIF5B labeled dysferlin-containing vesicles did not show long-range processive movement and are limited to local movements in resting L6 myotubes. These findings are consistent with reports describing processive and non-processive movements of kinesin-bound cargoes (36,37). Possible explanations for the non-processive behavior of a subpopulation of kinesin-containing dysferlin vesicles are that KIF5B may be bound to dysferlin-containing vesicles without sufficiently activating kinesin motor activity or without actively engaging microtubules (36) or perhaps the clustering of vesicles limits their motility or anchors them to another subcellular structure.

Dysferlin-containing vesicles undergo fusion to form large cytoplasmic vesicles following cellular wounding in L6 myotubes

L6 myotubes expressing dysferlin-eGFP were subjected to mechanical wounding using a finely pulled glass pipette and

analyzed for fusion of dysferlin-containing vesicles following wounding. Mechanical wounding reproducibly led to contracture and ultimately retraction of the myotube away from the wound site. This model of injury, in contrast to single point laser injury, is more analogous to the process of contraction-induced injury that occurs in muscle *in vivo* (38). In dystrophin-deficient dystrophic muscle, injurious lengthening contractions result in complete fiber tearing and the formation of contraction clots at the site of tearing (38). Interestingly, rather than accumulate specifically at membrane lesions in the L6 injury model, dysferlin-containing vesicles undergo rapid vesicle–vesicle fusion to form a population of extremely large dysferlin-containing vesicles throughout the cytoplasm of the myotube. In some cases the vesicles collapse on the membrane, but the majority of large vesicles remain in the cytoplasm and are stable for minutes following injury. This finding was somewhat surprising as our expectation was that dysferlin-containing vesicles would accumulate specifically at membrane lesions and fuse with the plasma membrane. The vesicle formation response was reminiscent of the 'vesicular plug' model of membrane resealing as has been previously documented in the urchin egg and crayfish medial giant axon, whereby endocytic and exocytic vesicles undergo fusion adjacent to membrane lesions and plug the lesion with minimal fusion with the plasma membrane (39, 40). Therefore, we propose that formation of large dysferlin vesicles may act as a vesicular plug which is, in itself, acting as a cellular 'contraction clot' capable of plugging large wounds in the plasma membrane of skeletal muscle cells. Additionally, it is interesting to speculate that cytoplasmic dysferlin-containing vesicles could play a different yet unappreciated role in response to wounding in muscle cells such as sequestering cytoplasmic components or damaged organelles that would otherwise harm neighboring cells. In fact, this idea is supported by recent evidence that the complement system is activated in dysferlin-null muscle, which contributes directly to disease progression, and may result from excess leakage of cellular contents following wounding (41).

Disruption of the functional linkage between dysferlin-containing vesicles and microtubules inhibits formation of large dysferlin-containing vesicles following wounding in L6 myotubes

Owing to the presence of KIF5B on dysferlin-containing vesicles and the requirement of microtubules for dysferlin-containing vesicle movement, we hypothesized that disruption of microtubules and/or kinesin motors would inhibit formation of large dysferlin-containing vesicles following wounding in L6 myotubes. We addressed this hypothesis by examining the effect of pharmacological disruption of microtubules or dominant negative inhibition of KIF5 motors on the formation of large dysferlin-vesicles following wounding in L6 myotubes. Both microtubule disruption and expression of dominant negative KIF5B significantly reduced the formation of large dysferlin-containing vesicles following wounding in differentiated L6 myotubes. These findings taken together with the fact that KIF5B is present on dysferlin-containing vesicles indicates that the functional linkage between KIF5B on dysferlin-containing vesicles and the microtubule lattice is critical for formation of large dysferlin vesicles following cellular wounding in L6 myotubes. There are several ways in which disrupting the link between microtubules and dysferlin-containing vesicles could inhibit large vesicle formation in muscle cells. It is possible that dysferlin-containing vesicles are transported throughout the cytoplasm via KIF5B prior to wounding and inhibition of KIF5B inhibits proper trafficking of dysferlin. However, the finding that dominant negative KIF5B does not markedly alter dysferlin localization indicates that transport of dysferlin-containing vesicles off the Golgi apparatus is intact, and cytoplasmic targeting of dysferlin-containing vesicles does not require KIF5B. One possible explanation for the dominant negative effect of KIF5B on vesicle formation is that KIF5B is required for movement of dysferlin-containing vesicles along microtubules following wounding, and this movement facilitates coalescence of adjacent dysferlin-containing vesicles. In this scenario, inhibition of KIF5B could impair large vesicle formation by disrupting proper movement of dysferlin-containing vesicles along microtubules following wounding. Unfortunately, analysis of motility following wounding in our assay was limited by the fact that wounding caused dramatic contracture of the myotube, resulting in movement of most cellular components. Regardless, our data indicate that the interaction between functional KIF5B motors on dysferlin-containing vesicles and microtubules is critical for formation of large vesicles following wounding.

Dysferlin-containing vesicles fuse with lysosomal compartments following wounding in L6 myotubes

The exact composition of dysferlin-containing vesicles, and membrane compartments involved in membrane repair in muscle have not been fully examined. Lysosomes have been implicated in membrane resealing across a variety of non-muscle cell types (30), but whether lysosomes are involved in dysferlin-mediated membrane resealing in skeletal muscle cells is not known. Lysosomal marker Lamp-2 accumulates around the nucleus of dysferlin-null myoblasts (13), indicating that loss of dysferlin may adversely affect lysosomal function. Furthermore, dysferlin is required for Fas-L-induced lipid raft clustering in endothelial cells, which is thought to be dependent on lysosomal fusion (42). Therefore, we sought to directly examine whether dysferlin-containing vesicles interact with lysosomal compartments following wounding in skeletal muscle cells. Live-cell imaging of L6 cells co-expressing dysferlin-eGFP and LGP120-mCh shows that dysferlin-eGFP and LGP120-mCh label independent populations of vesicles prior to wounding. Following wounding, dysferlin-containing vesicles undergo fusion with LGP120-mCh labeled compartments to form large vesicles in L6 myotubes. A previous study reported that lysosomal dispersion is impaired in cells isolated from KIF5B knockout mice, indicating that KIF5B may be required for motility of lysosomes (28). Our data indicate that lysosomal organization is not dramatically altered by dnKIF5B expression in differentiated L6 myotubes. This finding, taken together with the fact that KIF5B is present on dysferlin-containing vesicles prior to wounding indicates that the dominant negative effect on large vesicle formation is likely through direct impairment of dysferlin-containing vesicle function rather than an indirect effect on lysosomal function. These data support the novel assertion dysferlin-containing vesicles may interact to form large vesicles following wounding which may

contribute to membrane repair in L6 myotubes. Interestingly, knockout of synaptotagmin-VII, a dysferlin homolog necessary for lysosomal fusion, displays an inflammatory muscle myopathy (43), but whether loss of lysosomal function impairs resealing in muscle cells is not known. Furthermore, additional studies are needed to examine the exact contribution of lysosomal compartments to resealing in muscle and whether lysosomal behavior following wounding is impaired in dysferlin-deficient muscle cells.

MATERIALS AND METHODS

Mouse dysferlin isoform-1 (Gen Bank: NM_021469) was obtained as a kind gift from the Jain Foundation. A C-terminal fragment of dysferlin was isolated using a BSTBI-NOT1 fragment, and subcloned into a TOPO PCR 2.1 shuttle vector. The remaining N-terminal portion of dysferlin was excised using a KPNI-BSTBI digestion and inserted into the dysferlin C-terminus PCR2.1 vector. An eGFP fragment was generated using custom primers which generated a 5′SACII-eGFP-NOTI 3′ fragment in PCR 2.1. The GFP fragment was then excised using a SACII-NOTI digest, and inserted into the dysferlin-containing vector at the C-terminus. The entire dysferlin-GFP construct was then excised using a KPNI-NOTI digestion and inserted into a PCDNA 3.1+ vector for mammalian expression. Dysferlin-mCherry was generated using PCR amplification of mCherry with custom primers to generate a 5′SACII-mCherry-NOTI fragment. This fragment was then inserted into the aforementioned Dysferlin-eGFP construct using a SACII-NOTI digest. All dysferlin constructs were sequenced by the University of Michigan Sequencing Core. Motorless kinesins (containing the C-terminal stalk-tail region) are generally used as dominant negative inhibitors of kinesin function (44). Constructs encoding GFP or mCherry-labeled full-length rat KIF5 and dominant negative KIF5B (amino acids 568–964) were obtained as a kind gift from Dr Kristen Verhey. Previous work has shown that KIF5B and KIF5C interact, and that KIF5B can compensate for the loss of KIF5C (45), as such these constructs were used interchangeably throughout this manuscript. Thanks to Dr Kristen Verhey for the fluorophore-labeled kinesin and LGP120 constructs used in this study. Rat anti-α tubulin polyclonal antibody (AB6161) was obtained from ABCAM. Rabbit polyclonal antibody to PDI was obtained from Sigma. Mouse monoclonal antibody to GM130 was obtained from BD transduction labs. Nocodazole [Methyl *N*-(5-thenoyl-2-benzimidazolyl)carbamate] was obtained from Sigma Aldrich. Blebbistatin (1,2,3, 3a-tetrahydro-3a-hydroxy-6-methyl-1-phenyl-4H-pyrrolo[2,3-b] quinolin-4-one) was obtained from Toronto Research Chemicals, Inc. Alexa 488-conjugated phalloidin was obtained from Life Technologies. Anti-Lamp-1 antibody was obtained from ABCAM (ab24170). Lipofectamine™ 2000 reagent was used in all transfection experiments.

Cell culture and transfection

L6 myocytes were grown on 100 mm dishes under standard conditions at 37°C + 5% CO_2 in the presence of DMEM + 10% FBS + 1% P/S. Cells were subcultured using PBS wash followed by treatment with 0.25% trypsin-EDTA and plated on either 100 mm dishes for continued subculturing or 35 mm glass bottom dishes (MatTek) for live-cell imaging, or glass coverslips contained in 6-well dishes for immunofluorescence. L6 myocytes were transfected or co-transfected with cDNA(s) of interest using Lipofectamine 2000, according to the manufacturer's protocol. Following transfection, cells were switched to DMEM + 2% horse serum and allowed to differentiate for 4–8 days until cells formed elongated myotubes.

Immunofluorescence and image analysis

Differentiated L6 myotubes were fixed for 15 min in 3% paraformaldehyde, and permeabilized for 1 h in block solution containing 5% bovine serum albumin and 0.5% triton X-100. Following blocking, cells were incubated in block solution containing the appropriate titer of antibody at room temperature for 1.5 h. Following incubation in primary antibody, cells were washed and incubated in block solution containing the appropriate secondary antibody for 1 h. DAPI was used to stain nuclei in all immunofluorescence experiments. Images were obtained on the Deltavision® system using standard filter sets or a Leica SP8 confocal microscope with a 63× objective where indicated. For deltavision imaging, optical sections were generated at a thickness of 0.2 um for each channel and the resulting raw data was used to create projection images in SoftWoRx 1.3.0. Adobe Photoshop CS2 and Adobe Illustrator were used to compile images.

Live-cell imaging and quantification of dysferlin-containing vesicle transport

Dysferlin-eGFP-expressing L6 myotubes were switched from differentiation media to PBS + Ca^{2+} prior to imaging. Imaging was carried out on an Olympus BX-71 Deltavision® microscope, equipped with a climate control chamber to maintain 37°C and 5% CO_2. All imaging data were obtained on the Deltavision® live-cell system with an Olympus 60×, 1.4 numerical aperture objective, equipped with a PhotometricsCoolSnap HQ monochromatic camera. The SoftWoRx Explorer 1.3® imaging software was used in all experiments to analyze raw time-lapse data. The SoftWoRx 3.5.0® software was used to deconvolve time-lapse data when indicated, and was carried out using enhanced ratio with medium noise filtering unless otherwise noted. Quicktime movies or individual image files were generated from raw time-lapse data. Dysferlin-containing vesicle movement and nocodazole treatment: for analysis of dysferlin-containing vesicle movement, dysferlin-eGFP-expressing L6 myotubes were imaged at 250 ms exposure for 2 m prior to nocodazole treatment. To determine the effect of microtubule disruption on dysferlin-containing vesicle transport, cells were incubated in 750 mM nocodazole for 30 m and subjected to a second round of live-cell imaging for 2 min. Raw time-lapse images were then analyzed for dysferlin-containing vesicle movements >2 um in length using the Softworx® Particle Tracking software by an observer blind to the treatment group. Each individual motile vesicle was tracked through time and the total distance traveled was determined by manually assigning XY-coordinates to each motile vesicle at time-point. Each vesicle moving >2 um was counted as a movement, and the total number of movements was compared for each cell, prior to, and after treatment with nocodazole. Significance

was determined using Student's *t*-test. Velocities of individual dysferlin-containing vesicles (24 movements from 10 cells) were calculated by tracking individual motile vesicles and calculating the change in $x-y$ distance over time. These data should be taken as a close approximation, as our methodology does not account for displacement of vesicles within the *z*-plane.

Live-cell imaging of co-transfected L6 myotubes

To study multiple fluorescently tagged molecules, in single cells, experiments were designed to alternate imaging between each channel at 250 ms exposure for 2 min. The raw data for each channel were analyzed independently and in combination for vesicle motility and colabeling of dysferlin vesicles with molecules of interest. Movie files and images of individual and merged time-lapse data were generated for further analysis. Raw data and quicktime files were analyzed for colocalization, as well as the dynamic movement of both labels within the cell.

Live-cell membrane damage assay

To study the behavior of dysferlin-containing vesicles following membrane disruption, L6 myotubes expressing dysferlin-eGFP were subjected to live-cell imaging. Each cell was imaged in the GFP channel at 250 ms exposure for 2 min prior to membrane damage. Following initial imaging, each cell was re-visited and cells were wounded using a glass-pulled micropipette and imaged for 4–5 min following wounding. To damage myotubes, an MX140-R manual micromanipulator was mounted to the stage of an Olympus BX-71 Deltavision® microscope and equipped with a finely pulled glass pipette. Wounding was confirmed visually by the absence of fluorescence in the affected area, as well as hypercontracture of the myotube. Using these criteria over 90% of the cells that were assayed were characterized as wounded. Cells that did not hypercontract were re-wounded or discarded. Owing to movement artifact following membrane wounding, the *z*-axis was adjusted when necessary to highlight structures of interest. To quantify the vesicle formation response of dysferlin-eGFP-expressing myotubes to membrane disruption, raw time-lapse (.dv) files were analyzed using SoftWorx Explorer 1.3 for the formation of large dysferlin-vesicles following wounding. Any cell that formed dysferlin-containing vesicles with a visible lumen that was not present prior to wounding was characterized as a 'responder', and any cell that did not form vesicles was excluded from the analysis. For each responding cell, the total number of large (>2 um) damage-induced dysferlin-containing vesicles was quantified at a single time-point after vesicle formation had subsided. For nocodazole experiments, cells were incubated with DMSO or DMSO + 750 nM nocodazole for $\geq$30 min prior to wounding, imaged in the GFP channel at 250 ms exposure for 2 min prior to wounding, and 4–5 min following wounding. For dominant negative kinesin experiments, imaging alternated between GFP and dsRed channels at 250 ms exposure for 2 min to confirm expression of both constructs. Following initial imaging, each cell was wounded and imaged in the GFP channel alone at 250 ms exposure for 4–5 min. To determine the effect of nocodazole or dominant negative KIF5 on large vesicle formation, the average number of large vesicles (>2 μm) was quantified and compared with the respective control (DMSO or wt-KIF5, respectively). The data are presented as a bar graph in Figure 5B and 6C, and represent data collected from multiple independent experiments. Data are presented as a means $\pm$ SE and statistical analysis was carried out using a two-tailed *t*-test with a significance set at $P < 0.05$.

SUPPLEMENTARY MATERIAL

Supplementary Material is available at *HMG* online.

ACKNOWLEDGEMENTS

We would like to thank the members of the University of Michigan Microscopy and Image Analysis Laboratory (MIL) for all of its help with live-cell imaging. We would like to thank Dr Kristen Verhey for her generosity with the wild-type and dominant negative KIF5 constructs, as well as the construct encoding LGP120.

Conflict of Interest statement: none interest.

FUNDING

This work was supported by National Institutes of Health (HL-080388, HL-104893 to D.M.) and the American Heart Association (12PRE12050130 to J.M.).

REFERENCES

1. Hamer, P.W., McGeachie, J.M., Davies, M.J. and Grounds, M.D. (2002) Evans blue dye as an in vivo marker of myofibre damage: optimising parameters for detecting initial myofibre membrane permeability. *J. Anat.*, **200**, 69–79.
2. Bittner, R.E., Anderson, L.V.B., Burkhardt, E., Bashir, R., Vafiadaki, E., Ivanova, S., Raffelsberger, T., Maerk, I., Hoger, H., Jung, M. *et al.* (1999) Dysferlin deletion in sjl mice (sjl-dysf) defines a natural model for limb girdle muscular dystrophy 2b. *Nat. Genet.*, **23**, 141–142.
3. Bansal, D., Miyake, K., Vogel, S.S., Groh, S., Chen, C.-C., Williamson, R., McNeil, P.L. and Campbell, K.P. (2003) Defective membrane repair in dysferlin-deficient muscular dystrophy. *Nature*, **423**, 168–172.
4. Illarioshkin, S.N., Ivanova–Smolenskaya, I.A., Greenberg, C.R., Nylen, E., Sukhorukov, V.S., Poleshchuk, V.V., Markova, E.D. and Wrogemann, K. (2000) Identical dysferlin mutation in limb-girdle muscular dystrophy type 2b and distal myopathy. *Neurology*, **55**, 1931–1933.
5. Jaiswal, J.K., Marlow, G., Summerill, G., Mahjneh, I., Mueller, S., Hill, M., Miyake, K., Haase, H., Anderson, L.V.B., Richard, I. *et al.* (2007) Patients with a non-dysferlin miyoshi myopathy have a novel membrane repair defect. *Traffic*, **8**, 77–88.
6. Lek, A., Evesson, F.J., Sutton, R.B., North, K.N. and Cooper, S.T. (2011) Ferlins: regulators of vesicle fusion for auditory neurotransmission, receptor trafficking and membrane repair. *Traffic*, **13**, 185–194.
7. Liu, J., Aoki, M., Illa, I., Wu, C., Fardeau, M., Angelini, C., Serrano, C., Urtizberea, J.A., Hentati, F., Hamida, M.B. *et al.* (1998) Dysferlin, a novel skeletal muscle gene, is mutated in Miyoshi myopathy and limb girdle muscular dystrophy. *Nat. Genet.*, **20**, 31–36.
8. Piccolo, F., Moore, S.A., Ford, G.C. and Campbell, K.P. (2000) Intracellular accumulation and reduced sarcolemmal expression of dysferlin in limb-girdle muscular dystrophies. *Ann. Neurol.*, **48**, 902–912.
9. Han, R., Rader, E., Levy, J., Bansal, D. and Campbell, K. (2011) Dystrophin deficiency exacerbates skeletal muscle pathology in dysferlin-null mice. *Skeletal Muscle*, **1**, 35.
10. Klinge, L., Harris, J., Sewry, C., Charlton, R., Anderson, L., Laval, S., Chiu, Y.-H., Hornsey, M., Straub, V., Barresi, R. *et al.* (2010) Dysferlin associates with the developing t-tubule system in rodent and human skeletal muscle. *Muscle Nerve*, **41**, 166–173.
11. Belanto, J.J., Diaz-Perez, S.V., Magyar, C.E., Maxwell, M.M., Yilmaz, Y., Topp, K., Boso, G., Jamieson, C.H., Cacalano, N.A. and Jamieson, C.A.M.

(2010) Dexamethasone induces dysferlin in myoblasts and enhances their myogenic differentiation. *Neuromuscul. Disord.*, **20**, 111–121.
12. Sharma, A., Yu, C., Leung, C., Trane, A., Lau, M., Utokaparch, S., Shaheen, F., Sheibani, N. and Bernatchez, P. (2010) A new role for the muscle repair protein dysferlin in endothelial cell adhesion and angiogenesis. *Arterioscler. Thromb. Vasc. Biol.*, **30**, 2196–2204.
13. Demonbreun, A.R., Fahrenbach, J.P., Deveaux, K., Earley, J.U., Pytel, P. and McNally, E.M. (2011) Impaired muscle growth and response to insulin like growth factor 1 in dysferlin mediated muscular dystrophy. *Hum. Mol. Genet.*, **20**, 779–789.
14. Bi, G.Q., Alderton, J.M. and Steinhardt, R.A. (1995) Calcium-regulated exocytosis is required for cell membrane resealing. *J. Cell Biol.*, **131**, 1747–1758.
15. Bi, G.-Q., Morris, R.L., Liao, G., Alderton, J.M., Scholey, J.M. and Steinhardt, R.A. (1997) Kinesin- and myosin-driven steps of vesicle recruitment for Ca^{2+}-regulated exocytosis. *J. Cell Biol.*, **138**, 999–1008.
16. Steinhardt, R., Bi, G. and Alderton, J. (1994) Cell membrane resealing by a vesicular mechanism similar to neurotransmitter release. *Science*, **263**, 390–393.
17. Togo, T. and Steinhardt, R.A. (2004) Nonmuscle myosin iia and iib have distinct functions in the exocytosis-dependent process of cell membrane repair. *Mol. Biol. Cell*, **15**, 688–695.
18. Bement, W.M., Mandato, C.A. and Kirsch, M.N. (1999) Wound-induced assembly and closure of an actomyosin purse string in xenopus oocytes. *Curr. Biol.*, **9**, 579–587.
19. Abreu-Blanco, M.T., Verboon, J.M. and Parkhurst, S.M. (2011) Cell wound repair in drosophila occurs through three distinct phases of membrane and cytoskeletal remodeling. *J. Cell Biol.*, **193**, 455–464.
20. Han, R., Bansal, D., Miyake, K., Muniz, V.P., Weiss, R.M., McNeil, P.L. and Campbell, K.P. (2007) Dysferlin-mediated membrane repair protects the heart from stress-induced left ventricular injury. *J. Clin. Invest.*, **117**, 1805–1813.
21. Togo, T. (2006) Disruption of the plasma membrane stimulates rearrangement of microtubules and lipid traffic toward the wound site. *J. Cell Sci.*, **119**, 2780–2786.
22. Hernández-Deviez, D.J., Howes, M.T., Laval, S.H., Bushby, K., Hancock, J.F. and Parton, R.G. (2008) Caveolin regulates endocytosis of the muscle repair protein, dysferlin. *J. Biol. Chem.*, **283**, 6476–6488.
23. Hernández-Deviez, D.J., Martin, S., Laval, S.H., Lo, H.P., Cooper, S.T., North, K.N., Bushby, K. and Parton, R.G. (2006) Aberrant dysferlin trafficking in cells lacking caveolin or expressing dystrophy mutants of caveolin-3. *Hum. Mol. Genet.*, **15**, 129–142.
24. Roostalu, U. and Strähle, U. (2012) In vivo imaging of molecular interactions at damaged sarcolemma. *Dev. Cell.*, **22**, 515–529.
25. Huang, Y., Laval, S.H., van Remoortere, A., Baudier, J., Benaud, C., Anderson, L.V.B., Straub, V., Deelder, A., Frants, R.R., den Dunnen, J.T. *et al.* (2007) Ahnak, a novel component of the dysferlin protein complex, redistributes to the cytoplasm with dysferlin during skeletal muscle regeneration. *FASEB J.*, **21**, 732–742.
26. Azakir, B.A., Di Fulvio, S., Therrien, C. and Sinnreich, M. (2010) Dysferlin interacts with tubulin and microtubules in mouse skeletal muscle. *PLoS ONE*, **5**, e10122.
27. Cai, C., Masumiya, H., Weisleder, N., Matsuda, N., Nishi, M., Hwang, M., Ko, J.-K., Lin, P., Thornton, A., Zhao, X. *et al.* (2009) Mg53 nucleates assembly of cell membrane repair machinery. *Nat. Cell Biol.*, **11**, 56–64.
28. Tanaka, Y., Kanai, Y., Okada, Y., Nonaka, S., Takeda, S., Harada, A. and Hirokawa, N. (1998) Targeted disruption of mouse conventional kinesin heavy chain kif5b, results in abnormal perinuclear clustering of mitochondria. *Cell*, **93**, 1147–1158.
29. Wang, Z., Cui, J., Wong, W.M., Li, X., Xue, W., Lin, R., Wang, J., Wang, P., Tanner, J.A., Cheah, K.S.E. *et al.* (2013) Kif5b controls the localization of myofibril components for their assembly and linkage to the myotendinous junctions. *Development*, **140**, 617–626.
30. Reddy, A., Caler, E.V. and Andrews, N.W. (2001) Plasma membrane repair is mediated by Ca^{2+}-regulated exocytosis of lysosomes. *Cell*, **106**, 157–169.
31. Bashir, R., Britton, S., Strachan, T., Keers, S., Vafiadaki, E., Lako, M., Richard, I., Marchand, S., Bourg, N., Argov, Z. *et al.* (1998) A gene related to caenorhabditis elegans spermatogenesis factor fer-1 is mutated in limb-girdle muscular dystrophy type 2b. *Nat. Genet.*, **20**, 37–42.
32. Wenzel, K., Geier, C., Qadri, F., Hubner, N., Schulz, H., Erdmann, B., Gross, V., Bauer, D., Dechend, R., Dietz, R. *et al.* (2007) Dysfunction of dysferlin-deficient hearts. *J. Mol. Med.*, **85**, 1203–1214.
33. de Morrée, A., Hensbergen, P.J., van Haagen, H.H.H.B.M., Dragan, I., Deelder, A.M., 't Hoen, P.A.C., Frants, R.R. and van der Maarel, S.M. (2010) Proteomic analysis of the dysferlin protein complex unveils its importance for sarcolemmal maintenance and integrity. *PLoS ONE*, **5**, e13854.
34. Cai, Q., Gerwin, C. and Sheng, Z.-H. (2005) Syntabulin-mediated anterograde transport of mitochondria along neuronal processes. *J. Cell Biol.*, **170**, 959–969.
35. Cai, D., Verhey, K.J. and Meyhöfer, E. (2007) Tracking single kinesin molecules in the cytoplasm of mammalian cells. *Biophys. J.*, **92**, 4137–4144.
36. Kawano, T., Araseki, M., Araki, Y., Kinjo, M., Yamamoto, T. and Suzuki, T. (2012) A small peptide sequence is sufficient for initiating kinesin-1 activation through part of tpr region of klc1. *Traffic*, **13**, 834–848.
37. Farina, F., Pierobon, P., Delevoye, C., Monnet, J., Dingli, F., Loew, D., Quanz, M., Dutreix, M. and Cappello, G. (2013) Kinesin kifc1 actively transports bare double-stranded DNA. *Nucleic Acids Res.*, **41**, 4926–4937.
38. Claflin, D.R. and Brooks, S.V. (2008) Direct observation of failing fibers in muscles of dystrophic mice provides mechanistic insight into muscular dystrophy. *Am. J. Physiol. Cell Physiol.*, **294**, C651–C658.
39. McNeil, P.L. and Baker, M.M. (2001) Cell surface events during resealing visualized by scanning-electron microscopy. *Cell Tissue Res.*, **304**, 141–146.
40. Eddleman, C.S., Ballinger, M.L., Smyers, M.E., Godell, C.M., Fishman, H.M. and Bittner, G.D. (1997) Repair of plasmalemmal lesions by vesicles. *Proc. Natl Acad. Sci. USA*, **94**, 4745–4750.
41. Han, R., Frett, E.M., Levy, J.R., Rader, E.P., Lueck, J.D., Bansal, D., Moore, S.A., Ng, R., Beltrán-Valero de Bernabé, D., Faulkner, J.A. and Campbell, K.P. (2010) Genetic ablation of complement c3 attenuates muscle pathology in dysferlin-deficient mice. *J. Clin. Invest.*, **120**, 4366–4374.
42. Han, W.-Q., Xia, M., Xu, M., Boini, K.M., Ritter, J.K., Li, N.-J. and Li, P.-L. (2012) Lysosome fusion to the cell membrane is mediated by the dysferlin c2a domain in coronary arterial endothelial cells. *J. Cell Sci.*, **125**, 1225–1234.
43. Chakrabarti, S., Kobayashi, K.S., Flavell, R.A., Marks, C.B., Miyake, K., Liston, D.R., Fowler, K.T., Gorelick, F.S. and Andrews, N.W. (2003) Impaired membrane resealing and autoimmune myositis in synaptotagmin vii–deficient mice. *J. Cell Biol.*, **162**, 543–549.
44. Gelfand, V.I., Bot, N., Carolina Tuma, M. and Vernos, I. (2001) A dominant negative approach for functional studies of the kinesin II complex. *Methods Mol. Biol.*, **164**, 191–204.
45. Kanai, Y., Okada, Y., Tanaka, Y., Harada, A., Terada, S. and Hirokawa, N. (2000) Kif5c, a novel neuronal kinesin enriched in motor neurons. *J. Neurosci.*, **20**, 6374–6384.